J|A|C|S ARTICLES

Published on Web 10/21/2009

Electrospray Ionization Mass Spectrometry of Intrinsically Cationized Nanoparticles, $[Au_{144/146}(SC_{11}H_{22}N(CH_2CH_3)_3^+)_x(S(CH_2)_5CH_3)_y]^{x+}$

Christina A. Fields-Zinna, Rajesh Sardar, Christopher A. Beasley, and Royce W. Murray*

Kenan Laboratories of Chemistry, University of North Carolina, Chapel Hill, North Carolina 27599

Received August 17, 2009; E-mail: rwm@email.unc.edu

Abstract: Electrospray ionization triple-quadrupole mass spectrometry of ca. 1.6 nm diameter thiolate-protected gold nanoparticles has been achieved at higher resolution than in previous reports. The results reveal the presence of nanoparticles with formulas $Au_{144}L_{60}$ and $Au_{146}L_{59}$, present in the sample as a mixture. The improved resolution is based on lowering *m*/*z* by exchanging multiple $[-SC_{11}H_{22}N(CH_2CH_3)_3^+]$ ligands into the original $[-S(CH_2)_5CH_3]$ ligand shell. The nanoparticles are thus intrinsically cationized and appear as a series of 10+ to 15+ mass spectral peaks. The assigned state of charge was confirmed by a collision-induced dissociation measurement.

The chemistry and application of Au nanoparticles remains an active research field owing to a combination of their intrinsic scientific interest and their potential significant applications as, for example, sensors,[1,2] nanotechnology devices,[3−5] and nanomedical components.[6,7] Au nanoparticles offer advantages in ease of functionalization,[8−11] particularly for biomedical applications.[12−15] Very small (<2 nm) thiolate-protected clusters are an interesting focus of fundamental study as they can display unique size-dependent properties, both optical and electrochemical.[16−20]

Hanging over this field of Au nanoparticle research, however, is the slightly embarrassing question: Exactly what are they? The analytical chemistry needed to answer this question is in a primitive state. Nanoparticle identification has generally, by default, relied on methods lacking the needed compositional resolution and providing only average data sets: transmission electron microscopy (TEM),[21] X-ray photoelectron spectroscopy (XPS), and thermogravimetric analysis (TGA). The initial[23] mislabeling of the small nanoparticle $Au_{25}(SR)_{18}$[22] as $Au_{38}(SR)_{24}$[23] exemplifies the analytical limitations of TEM in particular. Improved compositional characterization of nanomaterials becomes steadily more important as their variety and range of applications evolve. Growing concern over nanoparticle toxicity[24,25] is also exacerbated by lack of compositional knowledge. Nanomaterials like thiolate-protected clusters can be properly understood only if they can be accurately identified and detailed chemical information obtained. Just as with a molecule, we want to gain as much information as we can about nanoparticles.

This paper reports a significant tactical advance in ionization of Au nanoparticles for electrospray ionization (ESI) mass spectrometry experiments, which (a) leads to a refinement of a

(1) Xu, X.; Wang, J.; Jiao, K.; Yang, X. *Biosens. Bioelectron.* **2009**, *24*, 3153–3158.
(2) Cobley, C. M.; Skrabalak, S. E.; Campbell, D. J.; Xia, Y. *Plasmonics* **2009**, *4*, 171–179.
(3) Koplin, E.; Simon, U. *Met. Nanoclusters Catal. Mater. Sci.: Issue Size Control* **2008**, 107–128.
(4) Puzzo, D. P.; Bonifacio, L. D.; Oreopoulos, J.; Yip, C. M.; Manners, I.; Ozin, G. A. *J. Mater. Chem.* **2009**, *19*, 3500–3506.
(5) Lee, K.; Hwang, Y.; Cheong, S.; Choi, Y.; Kwon, L.; Lee, J.; Kim, S. H. *Tribol Lett.* **2009**, *35*, 127–131.
(6) Liu, Y.; Miyoshi, H.; Nakamura, M. *Int. J. Cancer* **2007**, *120*, 2527–2537.
(7) Yaguee, C.; Moros, M.; Grazu, V.; Arruebo, M.; Santamaria, J. *Chem. Eng. J. (Amsterdam, Netherlands)* **2008**, *137*, 45–53.
(8) Hostetler, M. J.; Templeton, A. C.; Murray, R. W. *Langmuir* **1999**, *15*, 3782–3789.
(9) Selvakannan, P. R.; Mandal, S.; Phadtare, S.; Gole, A.; Pasricha, R.; Adyanthaya, S. D.; Sastry, M. *J. Colloid Interface Sci.* **2004**, *269*, 97.
(10) Gole, A.; Soman, C.; Sainkar, S. R.; Rao, M.; Sastry, M. *Bioconjugate Chem.* **2001**, *12*, 684.
(11) Sardar, R.; Shumaker-Parry, J. S. *Chem. Mater.* **2009**, *21*, 1167–1169.
(12) Oh, K. S.; Kim, R. S.; Lee, J.; Kim, D.; Cho, S. H.; Yuk, S. H. *J. Appl. Polym. Sci.* **2008**, *108*, 3239–3244.
(13) Daniel, M.-C.; Astruc, D. *Chem. Rev.* **2004**, *104*, 293–346.
(14) Eck, W.; Craig, G.; Sigdel, A.; Ritter, G.; Old, L. J.; Tang, L.; Brennan, M. F.; Allen, P. J.; Mason, M. D. *ACS Nano* **2008**, *2*, 2263–2272.
(15) Storhoff, J. J.; Mirkin, C. A. *Chem. Rev.* **1999**, *99*, 1849.
(16) Murray, R. W. *Chem. Rev.* **2008**, *108*, 2688–2720.
(17) Lee, D.; Donkers, R. L.; Wang, G.; Harper, A. S.; Murray, R. W. *J. Am. Chem. Soc.* **2004**, *126*, 6193–6199.
(18) Ingram, R. S.; Hostetler, M. J.; Murray, R. W.; Schaaff, T. G.; Khoury, J.; Whetten, R. L.; Bigioni, T. P.; Guthrie, D. K.; First, P. N. *J. Am. Chem. Soc.* **1997**, *119*, 9279–9280.
(19) Ruiz, V.; Colina, A.; Heras, M. A.; Lopez-Palacios, J. *Electrochem. Commun.* **2007**, *9*, 255–261.
(20) Sardar, R.; Beasley, C. A.; Murray, R. W. *Anal. Chem.* **2009**, *81*, 6960–6965.
(21) Wilcoxon, J. P.; Martin, J. E.; Provencio, P. *J. Chem. Phys.* **2001**, *115*, 998–1008.
(22) Tracy, J. B.; Kalyuzhny, G.; Crowe, M. C.; Balasubramanian, R.; Choi, J.-P.; Murray, R. W. *J. Am. Chem. Soc.* **2007**, *129*, 6706–6707.
(23) Donkers, R. L.; Lee, D.; Murray, R. W. *Langmuir* **2004**, *20*, 1945–1952.
(24) Pernodet, N.; Fang, X.; Sun, Y.; Bakhtina, A.; Ramakrishnan, A.; Sokolov, J.; Ulman, A.; Rafailovich, M. *Small* **2006**, *2*, 766–773.
(25) Murphy, C. J.; Gole, A. M.; Stone, J. W.; Sisco, P. N.; Alkilany, A. M.; Goldsmith, E. C.; Baxter, S. C. *Acc. Chem. Res.* **2008**, *41*, 1721–1730.

10.1021/ja906976w CCC: $40.75

formula reported in an earlier, lower resolution[26] mass spectrometry report; (b) confirms a theoretical prediction[27] of its composition; and (c) reveals the presence in the samples of a second, unexpected nanoparticle of a nearby composition. The two nanoparticles' compositions are $Au_{144}L_{60}$ and $Au_{146}L_{59}$, the former being the predicted one. The nanoparticle sample, previously called "Au_{140}"[28] or the "29 kDa" or "$Au_{144-146}(SR)_{50-60}$" nanoparticle,[29] was ligand-exchanged[8] with the thiol [$HSC_{11}H_{22}N(CH_2CH_3)_3^+$] ($HSTEA^+$), producing nanoparticles with mixed monolayers of $(-STEA^+)_x$ and $(-S(CH_2)_5CH_3)_y$ (SC6) thiolate ligands. Their ESI mass spectra reveal a mixture of two nanoparticles: $Au_{144}(STEA)_x(SC6)_y$ (where $x + y = 60$) and $Au_{146}(STEA)_x(SC6)_y$ (where $x + y = 59$). The advance is in making the nanoparticles "intrinsically highly ionized" by incorporating the stable cationic ligand $STEA^+$ into the nanoparticle organothiolate ligand shell.

"Au_{140}" nanoparticles have masses in the 35−40 kDa range. For proteins, such large masses are accessed in ESI mass spectrometry experiments by having substantial numbers of protonated amino acid base sites. The consequent large ionic charges (z) lower the mass/charge (m/z) ratio into ranges more conducive to good mass resolution in available instrumentation. The same tactic should apply to nanoparticles but in our hands has not been very successful when using dissociable ions such as protons or alkali metal ions. Nanoparticles with ligand shells terminated by $-CO_2H$[30] or short PEG chains $(OCH_2CH_2)_5$ (plus Na^+, K^+, Rb^+, or Cs^+)[22] have not thus far exhibited z values much above 4+ in ESI experiments. Hypothesizing that the dissociable ions do not build large z values due to electrostatic forces in the confined nanoparticle space in which they are held, we turned to affixing quaternary ammonium groups to the organothiolate ligand shell, relying on the stronger Au−thiolate bonds. We subsequently observed nanoparticle ions in charge ladders in which $z = 10+$ to 15+, due largely to their quaternary ammonium ($STEA^+$) termini.

Our experiments are built on an invaluable history of prior mass spectrometry investigations of nanoparticles,[31−35] including thiolate-protected gold clusters.[22,26,30,36−38] Laser desorption−ionization (LDI)[39] has been used to assign masses in nanoparticle mixtures but suffers from extensive fragmentation effects that make exact molecular formula assignment difficult. "Soft" ionization source mass spectrometry techniques (MALDI[37] and ESI[40]) have been more successful and have led to advances in detecting small nanoparticles.[37,40,41] $Au_{25}L_{18}$ has been studied with MALDI,[35,36] FT-ICR,[30] and various methods of ESI cationization, such as alkali metal coordination and carboxylic acid deprotonation,[22,30] and utilizing its innate core charge.[42] The crystal structure[43] of this particular nanoparticle has also been determined, confirming the assignments obtained from MS. Accessing more massive Au nanoparticle spectra by the tactic of substantially enhancing z values has not, however, heretofore been reported.

Experimental Section

Chemicals. Tetra-*n*-octylammonium bromide (Oct_4NBr, 98%), hexanethiolate (HSC_6H_{13}, HSC6), sodium borohydride ($NaBH_4$, 99%), 11-bromo-1-undecene ($Br(CH_2)_9CH{=}CH_2$, 95%), triethylamine ($(Et)_3N$, 99%), and tetrabutylammonium hexafluorophosphate ($TBAPF_6$, 99%) were obtained from Sigma-Aldrich. Certified ACS toluene, optima methylene chloride, optima methanol, optima acetonitrile, diethyl ether, hexane, and absolute ethanol (Fischer) were used as received. Hydrogen tetrachloroaurate trihydrate (from 99.999% pure gold) was prepared by a literature procedure and stored in a freezer at −20 °C. Water was purified with a Barnstead NANOpure system (18 MΩ). [$HSC_{11}H_{22}N(CH_2CH_3)_3^+$][$Cl^-$], or *N*,*N*,*N*-triethyl(11-undecenylmercapto)ammonium chloride ($HSTEA^+$), was prepared as follows: *N*,*N*,*N*-Triethyl-10-undecenylammonium bromide was synthesized via modification of a previously reported procedure.[44] 11-Bromo-1-undecene (12.2 mL, 52 mmol) was dissolved in 50 mL of ethanol, followed by the addition of triethylamine (25 mL, 170 mmol). The reaction mixture was then refluxed for 24 h. The volatiles were removed by rotary evaporation, and the product was redissolved in 20 mL of CH_2Cl_2. The product was collected through precipitation by hexane, resulting in a light yellow solid. ^{1}H NMR (CD_3Cl): 5.4−5.5 (m, 1H, $CH_2{=}CH$), 4.6−4.7 (m, 2H, $CH_2{=}CH$), 3.0−3.2 (q, 6H, $N(CH_2CH_3)_3$), 2.8−3.0 (m, 2H, $CH_2N(Et)_3$), 1.6−1.7 (m, 2H), 1.4−1.6 (m, 2H), and 1.2−1.4 ppm (m, 21H). *N*,*N*,*N*-Triethyl(11-undecenylmercapto)ammonium chloride was made by dissolving 3.34 g of *N*,*N*,*N*-triethyl-10-undecenylammonium bromide in 30 mL of CH_2Cl_2, followed by the addition of thioacetic acid (2 mL, 26 mmol). The reaction mixture was then irradiated under UV light for 24 h. The volatiles were removed under vacuum, and the solid was treated with Et_2O several times and dried to give a light yellow solid. The solid was then refluxed in 10% HCl (20 mL) for 3 h. After evaporation of solvent, the solid was crystallized from H_2O in the presence of decolorizing carbon. ^{1}H NMR (D_2O): 3.3−3.4 (q, 6H, $N(CH_2CH_3)_3$), 3.1−3.2 (m, 2H, $CH_2N(Et)_3$), 2.7−2.8 (t, 2H CH_2SH), 1.6−1.7 (m, 2H), 1.4−1.5 (m, 2H), and 1.2−1.4 ppm (m, 23H).

Synthesis of Nanoparticles. "Au_{140}" nanoparticles were synthesized as previously reported.[45] First, 3.1 g of $HAuCl_4$ was added to water and transferred from the aqueous phase to 45 mM Oct_4NBr in toluene. Next, 3.33 mL of hexanethiolate (HSC_6H_{13}), a 3:1 thiol:

(26) Chaki, N. K.; Negishi, Y.; Tsunoyama, H.; Shichibu, Y.; Tsukuda, T. *J. Am. Chem. Soc.* **2008**, *130*, 8608–8610.
(27) Lopez-Acevedo, O.; Akola, J.; Whetten, R. L.; Gronbeck, H.; Hakkinen, H. *J. Phys. Chem. C* **2009**, *113*, 5035–5038.
(28) Hostetler, M. J.; Wingate, J. E.; Zhong, C.-J.; Harris, J. E.; Vachet, R. W.; Clark, M. R.; Londono, J. D.; Green, S. J.; Stokes, J. J.; Wignall, G. D.; Glish, G. L.; Porter, M. D.; Evans, N. D.; Murray, R. W. *Langmuir* **1998**, *14*, 17–30.
(29) Schaaff, G. T.; Shafigullin, M. N.; Khoury, J. T.; Vezmar, I.; Whetten, R. L. *J. Phys. Chem. B* **2001**, *105*, 8785–8796.
(30) Tracy, J. B.; Crowe, M. C.; Parker, J. F.; Hampe, O.; Fields-Zinna, C. A.; Dass, A.; Murray, R. W. *J. Am. Chem. Soc.* **2007**, *129*, 16209–16215.
(31) Schaaff, T. G.; Whetten, R. L. *J. Phys. Chem. B* **2000**, *104*, 2630–2641.
(32) Whetten, R. L.; Khoury, J. T.; Alvarez, M. M.; Murthy, S.; Vezmar, I.; Wang, Z. L.; Stephens, P. W.; Cleveland, C. L.; Luedtke, W. D.; Landman, U. *Adv. Mater.* **1996**, *8*, 428–433.
(33) Jimenez, V. L.; Georganopoulou, D. G.; White, R. J.; Harper, A. S.; Mills, A. J.; Lee, D.; Murray, R. W. *Langmuir* **2004**, *20*, 6864–6870.
(34) McNeal, C. J.; Hughes, J. M.; Pignolet, L. H.; Nelson, L. T. J.; Gardner, T. G.; Fackler, J. P., Jr.; Winpenny, R. E. P.; Irgens, L. H.; Vigh, G.; Macfarlane, R. D. *Inorg. Chem.* **1993**, *32*, 5582–5590.
(35) Gaumet, J. J.; Strouse, G. F. *J. Am. Soc. Mass Spectrom.* **2000**, *11*, 338–344.
(36) Dass, A.; Dubay, G. R.; Fields-Zinna, C. A.; Murray, R. W. *Anal. Chem.* **2008**, *80*, 6845–6849.
(37) Dass, A.; Stevenson, A.; Dubay, G. R.; Tracy, J. B.; Murray, R. W. *J. Am. Chem. Soc.* **2008**, *130*, 5940–5946.
(38) Gies, A. P.; Hercules, D. M.; Gerdon, A. E.; Cliffel, D. E. *J. Am. Chem. Soc.* **2007**, *129*, 1095–1104.
(39) Templeton, A. C.; Wuelfing, W. P.; Murray, R. W. *Acc. Chem. Res.* **2000**, *33*, 27–36.
(40) Golightly, J. S.; Gao, L; Castleman, A. W., Jr.; Bergeron, D. E.; Hudgens, J. W.; Magyar, R. J.; Gonzalez, C. A *J. Phys. Chem. C* **2007**, *111*, 14625–14627.
(41) Schaaff, T. G.; Knight, G.; Shafigullin, M. N.; Borkman, R. F.; Whetten, R. L. *J. Phys. Chem. B* **1998**, *102*, 10643–10646.
(42) Negishi, Y.; Chaki, N. K.; Shichibu, Y.; Whetten, R. L.; Tsukuda, T. *J. Am. Chem. Soc.* **2007**, *129*, 11322–11323.
(43) Heaven, M. W.; Dass, A.; White, P. S.; Holt, K. M.; Murray, R. W. *J. Am. Chem. Soc.* **2008**, *130*, 3754–3755.
(44) Tien, J.; Terfort, A.; Whitesides, G. *Langmuir* **1997**, *13*, 5349–5355.

metal ratio, was added to the solution, which was stirred until clear. The solution was cooled to 0 °C, 3.8 g of $NaBH_4$ in 20 mL of ice-cold Nanopure water was added, and the solution was stirred vigorously for 1 h. Discarding the aqueous layer, the organic layer was washed three times with Nanopure water, and a viscous sludge resulted after rotary evaporation. The ethanol-soluble portion was collected by overnight extraction, filtered to remove larger nanoparticles, dried, and treated with acetonitrile to further remove smaller nanoparticles, excess ligands, and salts. The as-prepared "Au_{140}" is assumed to be neutral (zero core charge); the presence of some 1+ core charge species is possible but unlikely.

Ligand Exchanges. First, 0.02 mmol (or 6.4 mg) of $HSTEA^+$ was added to about 0.28 μmol (or 10 mg) of nanoparticle sample (ca. 80:1 ligands:nanoparticle mole ratio), dissolved in 1.48 mL of methylene chloride, and stirred for 30 min. Three products were formed according to the extent of ligand exchange with consequent solubilities: one was toluene soluble (minimal exchange), the second was toluene and water insoluble (medium extent of exchange) but methanol and methanol/CH_3CN soluble, and the third was water soluble (high extent of exchange). The "medium" exchange product was isolated and cleaned by washing several times with water and toluene to remove the free thiols, $HSTEA^+$ and HSC_6 thiol, respectively.

ESI-QQQ. Positive-mode spectra were obtained on a Micromass Quattro II triple-quadrupole (QQQ) mass spectrometer with a nanoelectrospray ionization source. The 8.75 μM nanoparticle sample was dissolved in a 70:30 acetonitrile:optima methanol solution (for solubility plus ESI compatibility). Four other experiments were performed with various solvent systems (70, 80, or 20 vol % CH_3CN, or 30 vol % CH_2Cl_2) as indicated in the Supporting Information, Figures S-1 and S-2. Instrumental parameters were adjusted for optimal detection of the molecular ions, precursor ions, and fragment ions, where the capillary was set at 1.4 V and the cone set at 27 V. Collision voltage set was around 70 for collision-induced dissociation (CID) conditions. For CID conditions, the sample was dissolved in 43% toluene, 29% methanol, and 28% acetonitrile, with a stoichiometric amount of $TBAPF_6$. Program resolution settings typical for detection of standard samples, such as proteins (>15), were too high for nanoparticle samples and resulted in distorted peaks that were difficult to resolve against background noise. Resolution settings affect peak broadness and mass accuracy. Successful resolution settings used here ranged from 10 to 13 on the equipment described above.

The spectra presented in this paper are limited to <4000 *m/z* by instrumental constraints. The data were smoothed using the Savitsky−Golay (17-point quadratic) method.[46] For high-resolution assignments of molecular formulas, the publicly available software, Molecular Weight Calculator, was used to produce simulated mass spectra for comparison to experiment. Note that in the figures, the designations $-STEA^+$ and −SC6 are shortened to T and C, respectively.

Results and Discussion

General Remarks. The ligand exchange of $-SC_{11}H_{22}N(CH_2CH_3)_3^+$ ($STEA^+$, or T in Figure 1) onto the ~1.6 nm diameter $-SC_6H_{13}$ (SC6, or C in Figure 1)-protected gold nanoparticle resulted in three approximately equal fractions, differing in solubility. We were not able to elicit spectra of the water- and toluene-soluble fractions. The fraction successfully studied in ESI mass spectrometry experiments was insoluble in toluene and water (permitting easy removal of excess ligands) but soluble in methanol. Solution mixtures with another solvent (70, 80, or 20 vol % CH_3CN, or 30 vol % CH_2Cl_2) with methanol were effective in producing ESI spectra (Supporting Information, Figures S-1 and S-2), along with varying resolution instrumental settings.

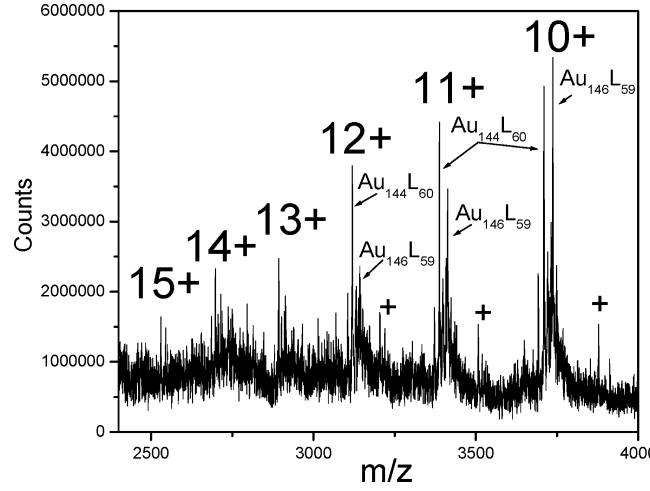

Figure 1. ESI-QQQ positive-mode spectrum of 1.6 nm diameter hexanethiolate-protected nanoparticle sample exchanged with $[HSC_{11}H_{22}(CH_2CH_3)_3N^+][Cl^-]$ ($STEA^+$, or T). Six charge states are detected, from 10+ to 15+, each including both $Au_{144}L_{60}$ and $Au_{146}L_{59}$. The charge *z* is due to the number of T ligands ($STEA^+$). Run in 70:30 MeCN:MeOH (optima grade), with no added electrolyte. This pattern of species was confirmed in five experiments as shown in the Supporting Information, Figures S-1 and S-2. (For + labels, see text.)

Figure 1 shows an ESI-QQQ mass spectrum of the nanoparticle sample in a 70:30 acetonitrile:methanol solution (no added electrolyte) at the highest obtained resolution setting. Spectra similar to Figure 1 were obtained in five different experiments using various solvent combinations (as above). The ion charges indicated on the figure were justified by a consistency of mass spacings between peaks, and between formula assignments and charge; for example, the $Au_{144}L_{60}^{10+}$ ion contains 10 $-STEA^+$ sites, and the $Au_{144}L_{60}^{11+}$ and $Au_{146}L_{59}^{11+}$ ions each contain 11 $-STEA^+$ sites. The charge assignment is further supported by a CID MS/MS experiment, described later. The detailed ion formula assignments are discussed in the next section. Charge "ladders" of peaks for differently charged macromolecules are well-known[47] for proteins, among others, but that in Figure 1 is the first reported for a nanoparticle.

The spectrum in Figure 1 shows prominent groups of peaks for 10+ to 15+ charge states, containing peaks for both $Au_{144}L_{60}$ and $Au_{146}L_{59}$ nanoparticles. The higher charge states (13+, 14+, 15+) exhibit lower peak intensities. That multiple charge states are present directly reflects the statistical nature of nanoparticle ligand exchanges, which has been demonstrated by mass spectrometric experiments on $Au_{25}L_{18}$ nanoparticles. Thus, a nanoparticle product of ligand exchange with the $HSTEA^+$ thiol having a certain Au atom count will maintain a constant Au and total ligand count but will be a mixture of nanoparticles bearing differing relative numbers of $-STEA^+$ and −SC6 ligands in, ideally, a binominal distribution.[48] The series of 10+ to 15+ peaks in Figure 1, each with a nanoparticle charge associated with the numbers of $-STEA^+$ ligands present, is a partial snapshot of such a distribution. The distribution seen in the spectrum has been truncated by the product solubility

(45) Hicks, J. F.; Templeton, A. C.; Chen, S.; Sheran, K. M.; Jasti, R.; Murray, R. W.; Debord, J.; Schaaff, T. G.; Whetten, R. L. *Anal. Chem.* **1999**, *71*, 3703–3711.
(46) Savitzky, A.; Golay, M. J. E. *Anal. Chem.* **1964**, *36*, 1627.
(47) Heck, A. J. R. *Nature Methods* **2008**, *5*, 927–933.
(48) Dass, A.; Holt, K.; Parker, J. F.; Feldberg, S. W.; Murray, R. W. *J. Phys. Chem. C* **2008**, *112*, 20276–20283.

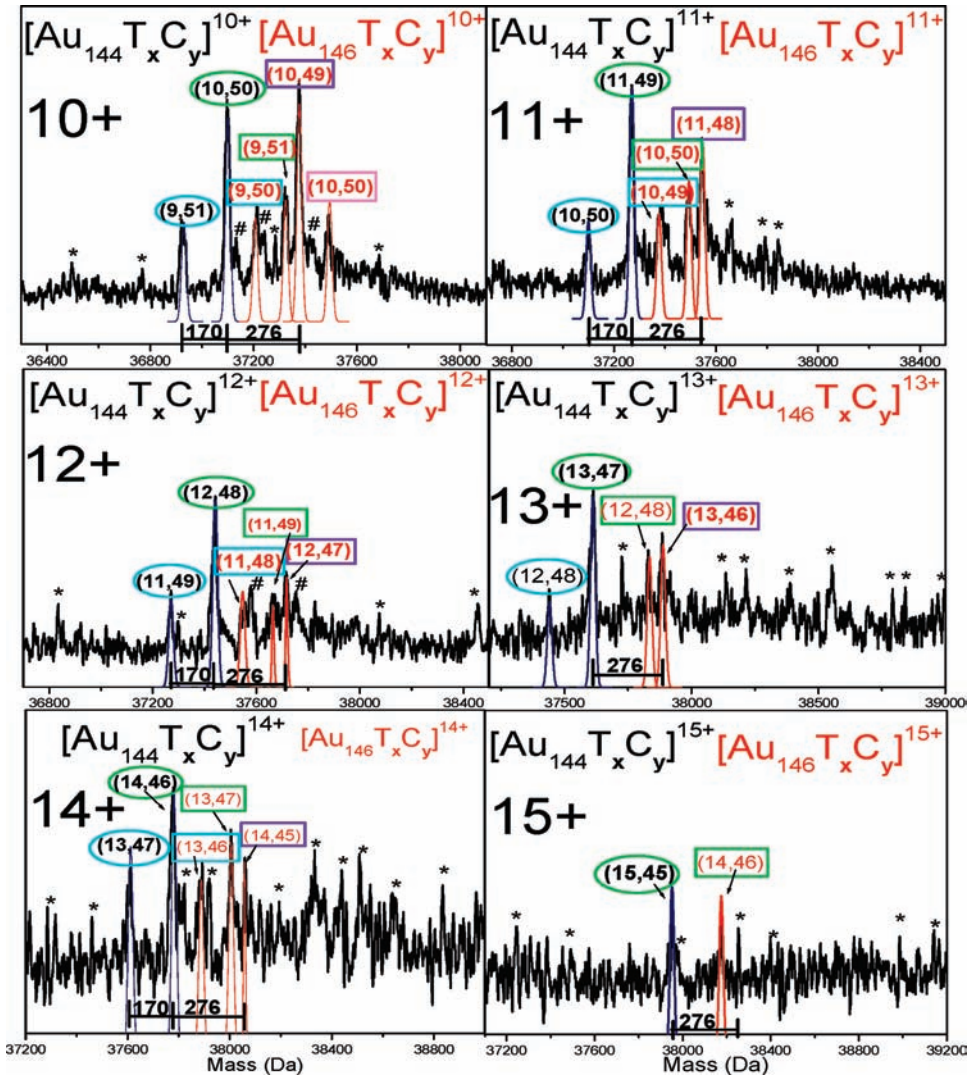

Figure 2. Spectral expansions of 10^+ to 15^+ ions, with formula assignments (x,y) and simulated peaks (dark blue and red). (Peaks labeled with * could not be assigned confidently due to poor signal-to-noise; for peaks labeled with # see text and Supporting Information, Figure S-3). Bars mark 170 Da mass spacings (mass difference of −SC6 (C) and $-SC_{11}H_{22}N(CH_2CH_3)_3^+$, $STEA^+$ or T) and 276 Da (mass difference for addition of two Au atoms and deletion of a C). No added electrolyte. (x,y) assignments are labeled by colored ovals for Au_{144} (black font) and rectangles for Au_{146} (red font); oval and rectangle colors indicate peaks with similar ligand compositions and core charges in the figure panels (see text).

differences, biasing against nanoparticles with larger and smaller numbers of −STEA ligands, and by the upper limit of instrumental m/z. Additionally, the apparent populations of nanoparticles in the spectrum are subject to individual ease of electrospray ionization and thus are not necessarily exactly representative of the "as prepared" sample.

Detailed Peak Assignments. Figure 2 shows spectral expansions of the groups of 10+ to 15+ ions, the formula assignments made for them, and peaks simulated (in dark blue and red) for those formulas. Table 1 summarizes the assignments.

The assignments of formula (and charge) were aided by the identification of particular mass spacings between peaks of like charge, e.g., the 170 Da difference in mass of the two ligands, $-STEA^+$ and −SC6, produces one recognizable peak spacing, and 276 Da is a spacing for peak formulas differing by mass equal to two Au minus one −SC6 ligand. These spacings are indicated by bars just below each spectrum and, as shown, are seen multiple times. This kind of peak spacing is a signature of exchange of one ligand for another with different mass, as shown in previous work[22,30,49] on $Au_{25}L_{18}$ nanoparticles (and confirmed by FTICR[30] and crystal structure determination).[43]

Figure 2 contains a great deal of information and will be explained in a stepwise fashion. The labels over the peaks in Figure 2 are either black or red, colors denoting nanoparticle ions having the general formulas $Au_{144}L_{60}$ (black) and $Au_{146}L_{59}$ (red). (x,y) labels the numbers of $-STEA^+$ (T) ligands (x) and −SC6 (C) ligands (y). Asterisks indicate peaks with poor signal-to-noise and repeatability that are therefore not confidently assigned.

Within the group of peaks labeled (black font) as $Au_{144}L_{60}$, two series of ligand compositions span the charge states seen in the different figure panels. Peaks in each series are visually connected to one another by differently colored *ovals* around the black (x,y) labels. In one series (green ovals), the Au nanoparticle core is formally neutral (Au_{144}^0): $(10,50)^{10+}$, $(11,49)^{11+}$, $(12,48)^{12+}$, $(13,47)^{13+}$, $(14,46)^{14+}$, and $(15,45)^{15+}$.

(49) Fields-Zinna, C. A.; Crowe, M. C.; Dass, A.; Weaver, J. E. F.; Murray, R. W. *Langmuir* **2009**, *25*, 7704–7710.

Table 1. Compositional and Charge Assignments of Species in Figures 1 and 2[a]

	charge state											
	10+		11+		12+		13+		14+		15+	
No. of Au atoms: 144												
no. of ligands (T + C = 60)												
T	10	9	11	10	12	11	13	12	14	13	15	n.o.
C	50	51	49	50	48	49	47	48	46	47	45	n.o.
core charge	0	1+	0	1+	0	1+	0	1+	0	1+	0	n.o.
m/z (obs)	3709.8	3692.5	3388.1	3372.6	3120	3105.9	2893.4	2910	2698.3	2686.3	2530.2	n.o.
m/z (calc)	3710.1	3693	3388.2	3372.8	3120.1	3105.9	2893.1	2910.3	2698.7	2686.5	2530.1	n.o.
No. of Au Atoms: 146												
no. of ligands (T + C = 59)												
T	10	9	11	10	12	11	13	n.o.	14	13	n.o.*	n.o.
C	49	50	48	49	47	48	46	n.o.	45	46	n.o.*	n.o.
core charge	0	1+	0	1+	0	1+	0	n.o.	0	1+	0	1+
m/z (obs)	3737.6	3721.1	3413.2	3398.5	3142.9	3129.5	2914.2	n.o.	2718.5	2706.6	n.o.*	n.o.
m/z (calc)	3737.7	3720.7	3413.2	3397.9	3143.1	3128.9	2914.4	n.o.	2718.4	2706.3	n.o.*	n.o.
No. of Au atoms: 146												
no. of ligands (T + C = 60)												
T	10	9	n.o.	10	n.o.	11	n.o.	12	n.o.	13	n.o.	14
C	50	51	n.o.	50	n.o.	49	n.o.	48	n.o.	47	n.o.	46
core charge	0	1+	0	1+	0	1+	0	1+	0	1+	0	1+
m/z (obs)	3748.9	3732.1	n.o.	3408.7	n.o.	3138.5	n.o.	2910	n.o.	2714.7	n.o.	2545
m/z (calc)	3749.4	3732.3	n.o.	3408.6	n.o.	3138.7	n.o.	2910.4	n.o.	2714.7	n.o.	2545

[a] Species are consistently observed in as many as five experiments (see Figures S-1 and S-2 in the Supporting Information). T is $-STEA^+$ and C is $-SC6$. "n.o." signifies not observed above the background noise. The (n.o.)* species was observed in a different experiment where electrolyte was added.

This series is generally the most intense member of each nanoparticle charge state. Note that the charges equal the numbers of cationic −STEA ligands. In the second series (sky blue ovals), the Au nanoparticle core is formally 1+ (Au_{144}^+): $(9,51)^{10+}$, $(10,50)^{11+}$, $(11,49)^{12+}$, $(12,48)^{13+}$, $(13,47)^{14+}$, and $(n.o.)^{15+}$ (n.o. signifies not observed above the background noise). The two series of ion peaks, $Au_{144}^0(10,50)^{10+}$, etc., and $Au_{144}^+(9,51)^{10+}$, etc., are related to one another in that one can envision the former as the parent of the latter by an electron loss (and a change in *z*) during the ESI process, i.e.,

$$[Au_{144}^0(STEA)_{10}(SC6)_{50}]^{10+} - e^- \rightarrow [Au_{144}^+(STEA)_{10}(SC6)_{50}]^{11+}$$

Any nanoparticles present in the "as prepared" sample with already 1+ core charges (thought unlikely to be plentiful) would contribute to the Au_{144}^+ series as well. The agreement between the observed and calculated *m/z* values of each of the peaks in the two $Au_{144}L_{60}$ series is generally excellent as seen in Table 1, where the calculated values are based on the simulations shown in Figure 2.

Turning to the red-labeled (*x*,*y*) peaks in Figure 2, these again correspond to several series of peaks that correspond to $Au_{146}L_{59}$ nanoparticles with different −STEA and −SC6 ligand compositions. Peaks in each series are labeled by colored *rectangles*. In one series (purple rectangles), the Au nanoparticle core is formally neutral (Au_{146}^0): $(10,49)^{10+}$, $(11,48)^{11+}$, $(12,47)^{12+}$, $(13,46)^{13+}$, $(14,45)^{14+}$, and n.o.*. (The n.o.* species was observed in a different experiment where electrolyte was added.) The second Au_{146} series (sky blue rectangles) is related to the first (Au_{146}^0) series by a core electron loss (Au_{146}^+): $(9,50)^{10+}$, $(10,49)^{11+}$, $(11,48)^{12+}$, $(n.o.)^{13+}$, $(13,46)^{14+}$, and $(n.o.)^{15+}$. The electron loss reaction can be written

$$[Au_{146}^0(STEA)_{10}(SC6)_{49}]^{10+} - e^- \rightarrow [Au_{146}^+(STEA)_{10}(SC6)_{49}]^{11+}$$

(Recall the above discussion of origin of 1+ core charges.) Again, the agreement between observed and calculated *m/z* values in Table 1 for the two series of $Au_{146}L_{59}$ peaks is generally very good. Further, peaks for both $Au_{144}L_{60}$ (black fonts) and $Au_{146}L_{59}$ (red fonts) were prominent under various instrumental resolution settings and were repeatedly observed in experiments using solvents containing different proportions of methanol and acetonitrile.

There are a few peaks in Figure 2 that are labeled as $Au_{146}L_{60}$ species, Au_{146}^0 $(10,50)^{10+}$ (pink rectangle), and a Au_{146}^+ charged-core series (green rectangles): $(9,51)^{10+}$, $(10,50)^{11+}$, $(11,49)^{12+}$, $(12,48)^{13+}$, $(13,47)^{14+}$, and $(14,46)^{15+}$. These peaks were not resolved from adjacent peaks and background in all experiments, so these assignments (also listed in Table 1) are more tenuous than the preceding. It is possible that $Au_{146}L_{60}$ species do exist in the sample but, under electrospray conditions, readily lose ligands to become $Au_{146}L_{59}$ nanoparticles. Further improvements in the ESI experiments will be required to be certain about the $Au_{146}L_{60}$ species. Another possible species, $Au_{145}L_{60\ or\ 61}$, is suggested by peaks in Figure 2 labeled "#", whose masses agree with simulations as shown in Supporting Information, Figure S-3. These peaks exhibit both 60 and 61 ligand counts and were not always resolved from adjacent peaks and background; again these constitute tenuous assignments.

As shown by the preceding analysis of Figure 2, far more certain in the ESI spectra are the unambiguous occurrences of $Au_{144}L_{60}$ and $Au_{146}L_{59}$ nanoparticles.

Some of the peaks in Figure 1, at *m/z* somewhat larger than the 10+ to 12+ sets of peaks, are labeled "+". These peaks appear to be ion adducts of nanoparticles and Cl^-; recall that the $HSTEA^+$ thiol was prepared as a chloride salt. Their assignments are shown in Supporting Information, Figure S-4; one is an ion pair with $Au_{146}L_{59}$ and another with $Au_{144}L_{60}$. There are two examples of $Au_{146}L_{60}$, but again these were not observed consistently in all five experiments.

Assignment Confirmation. A CID experiment was performed to confirm the multiple charging assignments and to support

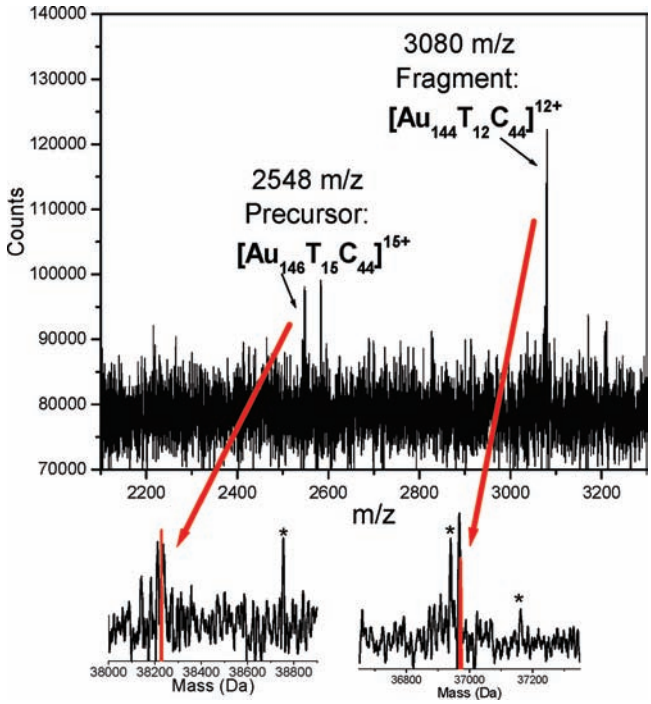

Figure 3. CID of 2548 *m/z* peak, which is $[Au_{146}(SC_{11}H_{22}(CH_2CH_3)_3N^+)_{15}(SC_6H_{13})_{44}]^{15+}$, or $Au_{146}T_{15}C_{44}$, shown in Figure 2 and labeled (15,44), which produces a fragment peak at higher *m/z* (around 3080 *m/z*), validating previous assignments of multiple-charging. $[Au_{146}T_{15}C_{44}]^{15+}$ (38 227 Da) loses $[Au_2T_3]^{3+}$ to produce $[Au_{144}T_{12}C_{44}]^{12+}$ (36 973 Da). Asterisks indicate apparent noise. This sample included tetrabutylammonium hexafluorophosphate ($TBAPF_6$) as electrolyte to enhance signal. Red arrows point to close-ups of precursor and fragment peaks. T is $-STEA^+$, and C is $-SC6$. Loss of Au_2L_3 equals a "staple" of $Au_{25}L_{18}$.[43]

the presence of Au_{146} nanoparticles, as shown in Figure 3. The ion $[Au_{146}(STEA^+)_{15}(SC_6)_{44}]^{15+}$ $(Au_{146}T_{15}C_{44})^{15+}$) was isolated and then fragmented, resulting in the detection of $[Au_{144}(STEA^+)_{12}(SC_6)_{44}]^{12+}$ $(Au_{144}T_{12}C_{44})^{12+}$), corresponding to a loss of $[Au_2(STEA^+)_3]^{3+}$. This was a difficult experiment given the lower intensities of the 15+ ions and poor S/N ratio, but the detected peaks shown at the bottom in Figure 3 match well with simulations. The Au_2L_3 fragment owes its charge to the three $-STEA^+$ ligands. Au_2L_3 has been recognized in CID of $Au_{25}L_{18}$ nanoparticles[50] as the apparent loss of an entire Au_2L_3 semi-ring. Theory[27] for the Au_{144} nanoparticle has predicted that the protecting semi-ring ligands are AuL_2. The cited CID study,[50] however, has also shown that semi-ring dissociation can involve rearrangement (and fragmentation even under non-CID conditions). Thus, Au_4L_4 fragments are seen for the $Au_{25}L_{18}$ nanoparticle which has exclusively Au_2L_3 semi-rings. The Figure 3 CID experiment is thus not inconsistent with the theory prediction. Additionally, the previously unknown precursor $Au_{146}L_{60}$ may have a different semi-ring population.

The CID experiment in Figure 3 was performed with electrolyte (a stoichiometric amount of tetrabutylammonium hexafluorophosphate ($TBAPF_6$)) added to the sprayed nanoparticle solution. A sensitivity of electrospray efficiency to electrolyte presence and concentration was uncovered late in this study. Some weak signals can become enhanced, such as that of the Figure 3 precursor ion $[Au_{146}(STEA^+)_{15}(SC_6)_{44})]^{15+}$, which was not well resolved in Figures 1 and 2. Further systematic exploration of this effect is needed to aid clarification of uncertain assignments mentioned above and to aid efforts to move to yet larger nanoparticles.

Conclusions

This study offers that "Au_{140}" nanoparticles contain a mixture of $Au_{144}L_{60}$ and $Au_{146}L_{59}$ and possibly other species. This material is more complex than previous studies have shown.

Acknowledgment. This research was supported in part by the National Science Foundation. The Molecular Weight Calculator is supported by the National Institutes of Health and the Department of Energy. We thank Dr. Sohrab Habibi, Department of Chemistry, University of North Carolina at Chapel Hill, for assistance with ESI mass spectrometric instrumentation.

Supporting Information Available: Supplementary mass spectra. This material is available free of charge via the Internet at http://pubs.acs.org.

JA906976W

(50) Fields-Zinna, C. A.; Sampson, J. S.; Crowe, M. C.; Tracy, J. B.; Parker, J. F.; deNey, A. M.; Muddiman, D. C.; Murray, R. W *J. Am. Chem. Soc.* **2009**, *131*, 13844–13851.